ACS APPLIED MATERIALS & INTERFACES

Research Article

www.acsami.org

Influence of Cross-linkers on the Cohesive and Adhesive Self-Healing Ability of Polysulfide-Based Thermosets

U. Lafont,*[,†,§] H. van Zeijl,[‡] and S. van der Zwaag[§]

[†]Material Innovation Institute, Mekelweg 2, 2600 GA, Delft, The Netherlands

[‡]DIMES, Electrical Engineering, Mathematics and Computer Science, Delft University of Technology, Mekelweg 4, 2628 CD, Delft, The Netherlands

[§]Novel Aerospace Materials, Aerospace Engineering, Delft University of Technology, Kluyverweg 1, 2629 HS, Delft, The Netherlands

Supporting Information

ABSTRACT: Synthetic systems with intrinsic self-repairing or self-healing abilities have emerged during the past decade. In this work, the influence of the cross-linker and chain rigidity on the healing ability of thermoset rubbers containing disulfide bonds have been investigated. The produced materials exhibit adhesive and cohesive self-healing properties. The recovery of these two functionalities upon the thermally triggered healing events has shown to be highly dependent on the network cross-link density and chain rigidity. As a result, depending on the rubber thermoset intrinsic physical properties, the thermal mending leading to full cohesive recovery can be achieved in 20−300 min at a modest healing temperature of 65 °C. The adhesive strength ranges from 0.2 to 0.5 MPa and is fully recovered even after multiple failure events.

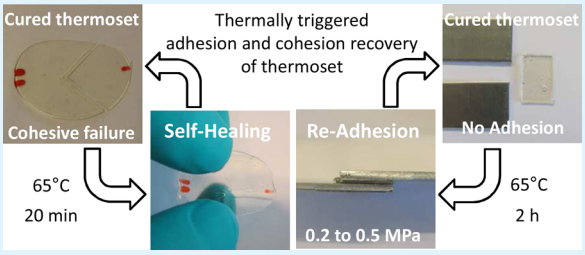

KEYWORDS: *self-healing polymers, reversible adhesion, thermal mending, cohesion, polysulfide, thermoset*

INTRODUCTION

The need for materials that are very reliable and durable has been the main motivation to the development of self-healing materials.[1] For a decade, the newly emerging self-healing concepts in material science have been mainly applied for structural materials that have to carry mechanical loads[2] or materials that have a protective function.[3,4] For these applications, the scale of the damage to be healed lies in the millimeter to submillimeter range. Downscaling the self-healing concept to heal damages from micrometer to submicrometer range will be of great interest for systems where the main failure mode differs from structural failures. For example, restoration of interfacial properties (adhesion) and conductivity (electronic, ionic, or thermal) could be of great interest for many applications.[5]

There are basically two well-established ways to develop self-healing concepts in materials. The first one is based on the integration of discrete mono-, bi-, or tridimensional containers (layers, capsule, fibers, or vascular network)[6−23] loaded with active components into the matrix material. In this approach, there is a physical separation between the material responsible for the healing action and the material responsible for the intended functionality. The second approach relates to the development of so-called intrinsically self-healing materials or mendable polymers,[24] that is, materials containing dynamic bonds that can restore their chemical or physical bonds under the influence of a nondisruptive external stimulus.[25] In this approach the "matrix" material combines both the healing and the functional role. Some of the most elegant routes to achieve intrinsic healing in polymeric materials are Diels−Alder and retro-Diels−Alder-based reactions,[26−34] hydrogen bonding in supramolecular network,[35−38] coordination complex,[39−41] disulfides based chemistries,[42−44] ionic clusters in ionomers,[45−49] or more recently perfluorocyclobutane based chemistries,[50] [4 + 4] dimerization of anthracene,[51,52] photopolymerisation of coumarin,[53] maleimide chemistry,[54] alkoxyamine dissociation-association,[55] and trans-esterification reaction.[56]

Thermosets are widely use materials that once cured do not recover any of their initial properties. In this respect, many effort have been devoted to implement self-healing functionalities based on intrinsic self-healing abilities in thermoset-based materials. The recovery of their cohesive and adhesive functionalities will be great advantage to increase their service lifetime and has been recently the main focus point in the development of self-healing materials.[57−60] Among the most attractive chemistries explored to create such materials the disulfide route particularly is promising and easy to process. In biological systems, this mechanism underlies the construction and stabilization of highly ordered proteins.[61] The cleavage of a sulfur−sulfur bond can be realized under several conditions, like oxido-reduction[62,63] and thermal scission,[64] but can also

Received: September 4, 2012
Accepted: October 19, 2012
Published: October 19, 2012

result from mechanical stress[65,66] or photoirradiation.[67] In any of these cases the creation of thiolate anions or sulphenyl radicals is involved which leads to local molecular rearrangements and the subsequent creation of new covalent bonds. On the other hand, it has been suggested that disulfide bonds can undergoes thermodynamically driven metathesis reactions (exchange reaction) in which two S−S bonds are disrupted and reform.[43,67,68] In this respect, any molecules or polymer where at least one disulfide bond is present can be eligible to exhibit this dynamic bonding/debonding ability. Regardless of the detailed mechanism the self-healing ability will be highly dependent on the density and mobility of disulfide bonds available within the polymeric network. In the same way as the thermoset's mechanical properties are tuned by changing the cross-linking density and number of branches per cross-link unit, the self-healing response of a thermoset polymer based on the presence of S−S bonds is expected to be sensitive to the prevailing network. As a result, tuning of the material response could be achieved by simply changing the network using different cross-linkers. In the field of intrinsic self-healing materials, the effect of the network cross-link density on the healing response has not yet been investigated. Therefore, in our work we aim to present a material in which the mechanical integrity is recovered (self-healed) re-establishing cohesion within the material as well as adhesive bonding to an Al alloy substrate. The formulation and characterization of a polymeric matrix presenting two self-healing properties (cohesion and adhesion) based on thermally triggered disulfide exchange reactions is presented in this work. The effect of two different cross-linkers with different chain length on the self-healing cohesive and adhesive behavior of thermosets in the rubbery phase has been investigated.

EXPERIMENTAL SECTION

Chemicals. The self-healing matrix used in this research is a thermoset epoxy resin presenting disulfide bonds in its structure. The epoxidized polysulfides Thioplast EPS25 (640 g/equiv) and EPS70 (310 g/equiv) were provided by AkzoNobel BV. An epoxy resin EPIKOTE 828 consisting of Polybisphenol A-co-epichlorohydrin (~188 g/equ.) provided by Momentive Specialty Chemical BV has been used as the reference compound. Two different cross-linkers presenting different thiol reactive functionality have been used in this study. The first one, with four thiol functions per cross-linker unit, Pentaerythritol tetrakis(3-mercaptopropionate) (~122 g/equiv), was purchased from Aldrich. This compound will be denoted here as 4-SH. The second one, presenting three thiol functions per cross-linker unit, is Capcure 3−800 (~270 g/equ) and was provided by Cognis GmbH. This compound will be denoted as 3-SH here. The precursors molecular structure are presented in Scheme 1.

The cross-linking reaction was catalyzed using 1 wt % of 4-dimethylaminopyridine (DMAP) from Aldrich. All chemicals were used as received. The mass per equivalent value used are the one provided on the product data sheet.

Preparation of the Polysulfide-Based Self-Healing Rubber Thermoset. The amount of cross-linker used has been calculated to provide the stoichiometric amount of reactive cross-linking functions with respect to the amount of reactive epoxy groups. The equivalent molar ratios of resin/cross-linker are 2 and 1.5 using 4-SH or 3-SH cross-linker, respectively. All precursors (epoxy resin, cross-linker, and catalyst) were mixed in a polypropylene container for 2 min using a speed mixer at 2000 rpm. The resulting mixes were transferred to a 1 mm thick mold and then cured at 65 °C for 2 h. Three different sample per type of cross-linker were produced using pure EPS25 or a 50/50 mol % mix of ESP25 and ESP70 or pure EPS70. The samples produced were labeled as follow: ESP25 mol %-EPS70 mol %-cross-linker type. The compositions of the different resins produced for this study are reported in Table 1. The resulting cured materials were used as starting materials to perform all characterization tests as well as cohesion and adhesion recovery tests. The nonself-healing samples used as reference consist of pure Epikote cured with a stoichiometric amount of 3-SH or 4-SH cross-linker, denoted Epikot-3SH and Epikote-4SH, respectively.

Scheme 1. Molecular Structure of EPS25 and EPS70 Polysulfide and Cross-linker Precursors

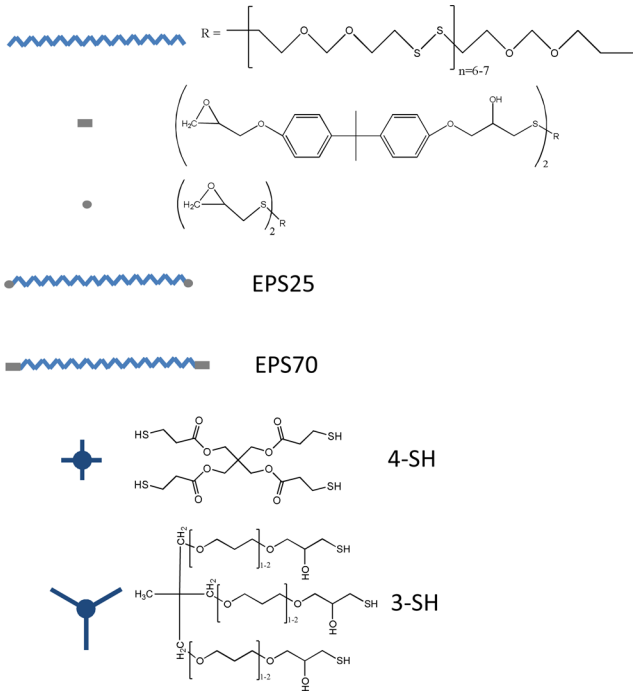

Table 1. Composition of the Different Polysulfide Containing Materials Produced Using the 4-SH or 3-SH Type Cross-Linker

	resin content (mmol)-(equiv)-(g)		cross-linker content (mmol)-(equiv)-(g)	
samples[a]	EPS25	EPS70	4-SH	3-SH
100-0-4SH	10-0.02-12.8		5-0.02-2.44	
50-50-4SH	5-0.01-6.4	5-0.01-3.1	5-0.02-2.44	
0-100-4SH		10-0.02-6.2	5-0.02-2.44	
100-0-3SH	10-0.02-12.8			6.66-0.02-5.40
50-50-3SH	5-0.01-6.4	5-0.01-3.1		6.66-0.02-5.40
0-100-3SH		10-0.02-6.2		6.66-0.02-5.40

[a]Sample labeling: ESP25 mol %-EPS70 mol %-cross-linker type.

FTIR-ATR Experiments. The cross-linking reaction related to the thermoset formation was monitored by infrared spectroscopy using a PerkinElmer Spectrum 100 FTIR-ATR on the cured samples. To get a bulk investigation of the molecular vibration of the sample and discard surface passivation, the produced materials were investigated by facing a freshly cut part of the sample on the crystal of the FTIR-ATR device.

TGA Experiments. Thermogravimetric analyses were performed by adding 10 mg of sample in a PerkinElmer Pyris Diamond TG/DTA. The sample were heated under air flow from room temperature to 550 °C at a rate of 10 K/min.

DSC Experiments. Differential scanning calorimetry tests were done using 5−10 mg of sample and a PerkinElmer Sapphire DSC using an heating rate of 10 K/min under N_2 atmosphere. For the EPS based materials, the samples were first cooled to −60 °C then heated to 25 °C. For Epikote-based material, the temperature range used was −20 to 120 °C and 25 to 120 °C for the 3-SH and 4SH material,

dx.doi.org/10.1021/am301879z | ACS Appl. Mater. Interfaces 2012, 4, 6280−6288

respectively. For each sample 2 cool-heat run have been performed and the T_g values have been extracted using the inflection point of the DSC curves on the second heating run.

Density Measurements. Density were performed using the Archimedean immersion method in water at room temperature.

Cohesion Recovery Tests. To investigate the cohesive healing ability, the samples were fully cut using a clean razor blade. The pieces of material were put back together and placed between two glass slides. The resulting width of the gaps spans from 100 to 400 μm. The cohesive healing ability has been investigated at 65 and 100 °C. Every 10 min, the samples were taken out from the oven and the cohesion recovery was monitored using a Leica optical microscope. A graphical analysis of the micrographs was performed to determine the variation of the cut width for a single sample at multiple locations as well as the average cut area for each sample. These values, which obviously are a function of the healing time (t) were compare to the initial values at t = 0 min. The healing efficiency was calculated as follows: efficiency = $(1 - V_t/V_{t0})$. This procedure was repeated until full mending.

Lap-Shear Experiments. Single lap shear tests using aluminum alloy 6082-T6 plates were performed at room temperature using a Zwick/Roell 250 tensile tester to determine adhesive healing in a more quantitative manner. For adhesive samples preparation, a known surface of already cured resin (12.5 × 25 mm^2, thickness 1 mm) was sandwiched between two identical aluminum plates ($L \times W \times T$ = 100 × 25 × 2 mm^3) with an overlap length of ∼12.5 mm. The adhesion was promoted by a 2 h thermal treatment at 65 or 100 °C. During the thermal treatment the adhesive and the two parts of the sample were kept in contact using a paper clip (Supporting Information Figure S3). Prior testing, the samples were allowed to cool down to room temperature for a minimum of 2 h. The overlapping area was measured and controlled before each test. The elongation rate used was fixed at 1 mm/min for all measurement. The tests were stopped after complete failure meaning that the bond line has been broken and the two aluminum plates were completely separated. Five experiments were performed per sample and all experiments showed a consistent behavior. After the failure, the sample ends were repositioned carefully to recover the same bond area and the thermal treatment was repeated followed by the lap shear test using the same protocol. Each thermal treatment at a given temperature that aim to promote the recovery of adhesion will be further denoted as an "healing event".

RESULTS AND DISCUSSION

The completion of the cross-linking process involving the reaction of the thiol functions of the cross-linker with the oxirane rings of the epoxidized polysulfide has been monitored by infrared spectroscopy. The complete disappearance of the vibration band at 2560−2568 cm^{-1} related to the S−H stretching demonstrated that for all materials produced, all cross-linkers did react fully (Figure 1). Another way to check and further confirm the complete reaction of the precursors is to monitor the disappearance of the oxirane ring stretching. For the EPS25 based material after curing no oxirane ring stretching vibrations at 842−863 cm^{-1} were detected. For the aromatic resins EPS70 the oxirane related IR band overlap with the strong IR band related to the aromatic C−H out of plane bending at 830 cm^{-1} and cannot be monitored. However, for the EPS70 based system, the disappearance of the thiol vibration could be monitored, which confirms that the oxirane ring-opening reaction took place during cross-linking.

To further confirm the completeness of the cross-linking reaction in our samples after the initial curing step at 65 °C for 2 h, additional DSC experiments were performed from room temperature to 120 °C. Any further cross-linking reaction would have manifested itself as an exothermic event on the DSC curves. None of our samples showed any sign of further cross-linking once cured (Supporting Information Figure S3). As we aim to promote the healing using a thermal stimulus, the

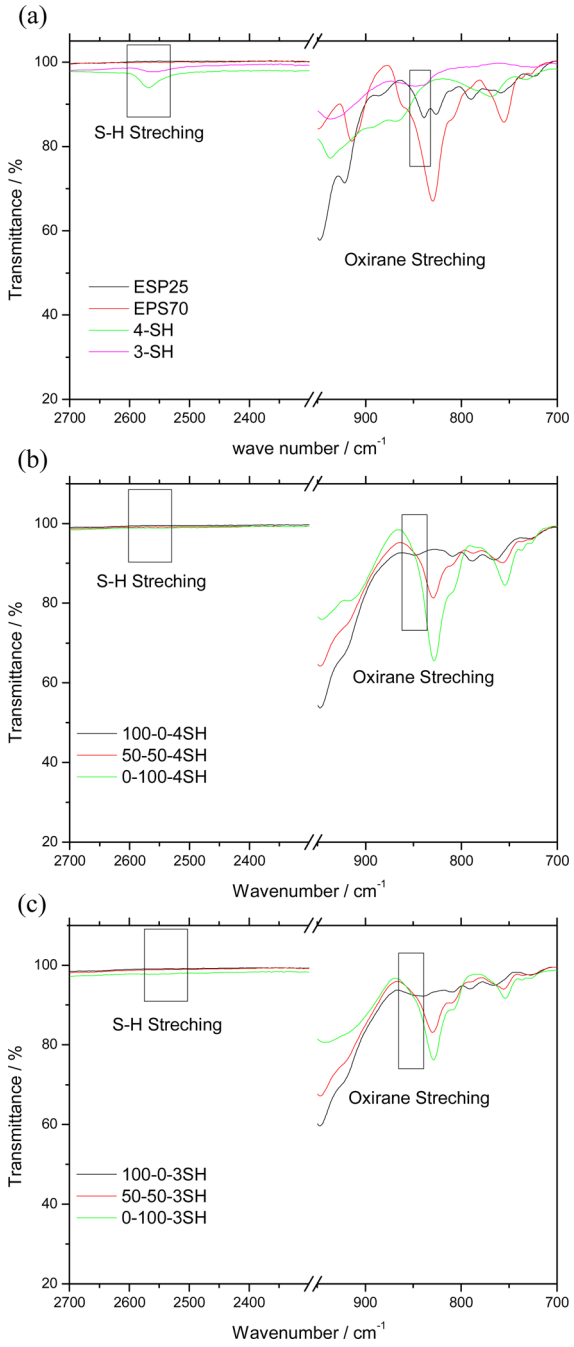

Figure 1. FTIR spectra of the precursors (a), the resulting resin after curing using 4-SH (b), and 3-SH (c) cross-linker.

thermal stability and weight loss of the produced thermoset has been investigated by TGA (Figure 2). The decomposition onset temperature and the temperature at which 1% and 10% weight loss occurred for the polymers produced are listed in Table 2. The thermal stability is clearly influenced by the type of cross-linker. The cross-linker used differs in their branching and chain length. Using a short chain tetrathiol as cross-linker (4-SH), the samples shows a 1% mass loss at 130 °C for a pure aliphatic (EPS25) resin. This value is increased to 160 °C upon blending with EPS70 resin. Using a trithiol cross-linker (3-SH) with longer chains, the 1% mass loss occurs at 140 °C for the EPS25, the blend and the EPS70 resin. The reference systems based on the Epikote resin show much higher degradation onset temperatures.

dx.doi.org/10.1021/am301879z | ACS Appl. Mater. Interfaces 2012, 4, 6280−6288

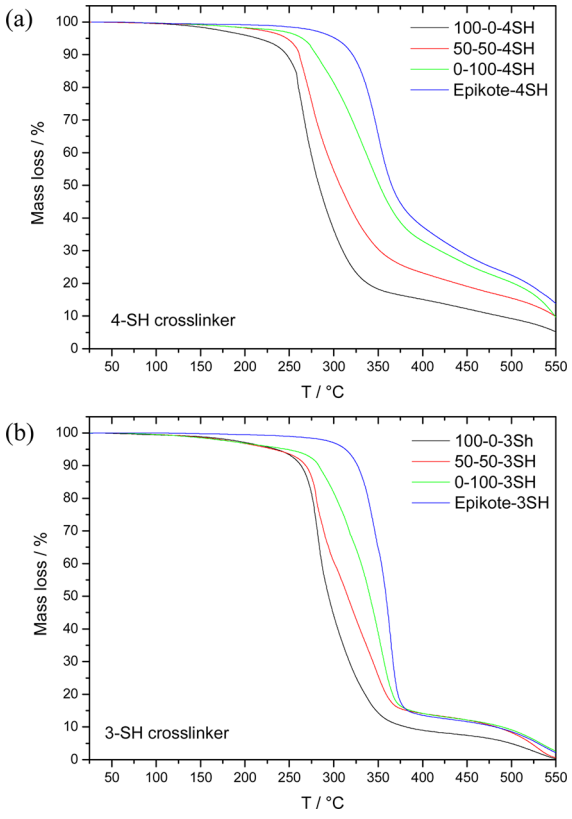

Figure 2. TGA of the (a) 4-SH and (b) 3-SH based materials.

Table 2. Thermo-oxidative Properties, T_g, and Density Values of Polysulfide and Epikote-Based Cross-linked Polymers

samples	1% weight loss (°C)	10% weight loss (°C)	T_g (°C)	density (g.cm^{-3})
100-0-4SH	130	247	−46	1.29123
50-50-4SH	160	261	−33	1.28086
0-100-4SH	160	280	−3.6	1.25586
Epikote-4SH	220	320	55	1.26511
100-0-3SH	140	262	−40	1.25220
50-50-3SH	140	268	−33	1.22908
0-100-3SH	140	283	−11	1.18778
Epikote-3SH	247	326	13	1.13686

The implementation of aromatic functionalities in the material gradually improves the thermal resistance of the material which is in line with theoretical expectation. The decomposition temperature is gradually increased from 247 to 280 °C for blends ranging from pure EPS25 to pure EPS70 using 4-SH as cross-linker, whereas these values are increased from 262 to 283 °C using 3-SH type cross-linker. The materials made using Epikote having the highest aromatic functionality in its backbones exhibit a higher thermal stability and comparable decomposition temperature of 320 and 326 °C for 4-SH and 3-SH cross-linker, respectively. The glass transition temperature (T_g) of the produced material deduced from DSC experiments are presented in Table 2. The materials using 3-SH as cross-linker exhibit an increase in their T_g from −40 to −11 °C with increasing amount of EPS70 in the blend. Using 4-SH cross-linker the T_g is increased from −46 to −3.6 °C. The T_g variation range is around 42.4 °C using 4-SH cross-linker whereas this variation range is reduced to 29 °C in average using 3-SH cross-linkers. Using the aliphatic based resin, the lowest T_g is achieved for the 4-SH cross-linker whereas when using the aromatic based resin the lowest T_g is achieved for the 3-SH cross-linker. The cross-linker type does not affect the T_g of the blended material containing an equivalent molar amount of aliphatic and aromatic resins.

The cohesive healing of the produced material has been investigated upon thermal mending at low (65 °C) and high (100 °C) temperatures. These two temperatures are below the decomposition temperature of all produced materials. The results of the thermally triggered cohesion recovery are plotted in Figure 3. The cohesion recovery follows an exponential recovery as function of time. All experimental point could be fitted using a first order exponential function. The fit results are plotted in Figure 3 using a full line and dotted line for the 4-SH and 3-SH based materials, respectively. Using the 4-SH cross-linker, the ESP25 based material present a very fast cohesive healing. A full cohesive recovery is achieved within 20 min for both temperatures. As soon as aromatic based resin are introduced into the blend, the healing time at 65 °C increases to 150 and 240 min for the 50-50-4SH and 0-100-4SH (pure EPS70) material, respectively. At high healing temperature this specific time drops to 60 and 80 min for the 50-50-4SH and 0-100-4SH material, respectively. By decreasing the network density using 3-SH cross-linker, the specific time to reach a full cohesive healing is the same (20 min) for the pure aliphatic material for both healing temperatures. Compare to the material made using 4-SH, when the amount of EPS70 is increase, the healing time is also increased to 240 min for 50-50-3SH and to 300 min for the pure EPS70. At low healing temperature the gradual implementation of aromatic segments (more rigid segments) in the material have a negative effect on the cohesion recovery time. However, this effect is minimized when tetra-functional cross-links are used. At high healing temperatures both effects related to the cross-linkers and the increases in aromatic segment fraction are minimized and the 3-SH based materials behave almost like the 4-SH ones. It is interesting to note that for the pure aliphatic material, there are no differences in the healing time regardless the cross-linker and healing temperature used. In this case, the high intrinsic mobility of aliphatic chain of the resin masks the difference in cross-link density. The reference materials based on Epikote resin that do not contain any S−S bonds in their structure did not exhibit any thermal mending irrespective of the cross-linkers, the temperature used and the healing time. Opposite to this, all materials containing S−S bonds have shown to restore a cohesive integrity between each other regardless of the cross-linker and backbone used (Supporting Information Figure S5).

The shorter healing time is the consequence of the enhanced molecular mobility and an healing temperature far above the glass transition temperature is thus favorable to promote a cohesive recovery. The effect of the T_g on the cohesive healing efficiency is plotted in Figure 4 where the time related to a full cohesion recovery is plotted as function of the difference between the healing temperature and T_g. The reference material was not plotted as no cohesion recovery occurs at 65 or 100 °C. However, at 100 °C the difference between the healing temperature and the T_g of Epikote-3SH and Epikote-4SH are 77 and 45 °C, respectively. These differences are comparable for those of the pure EPS70 based materials healed at 65 °C that show thermally triggered cohesion recovery. In case the degree of cohesion recovery was only related to the

dx.doi.org/10.1021/am301879z | ACS Appl. Mater. Interfaces 2012, 4, 6280−6288

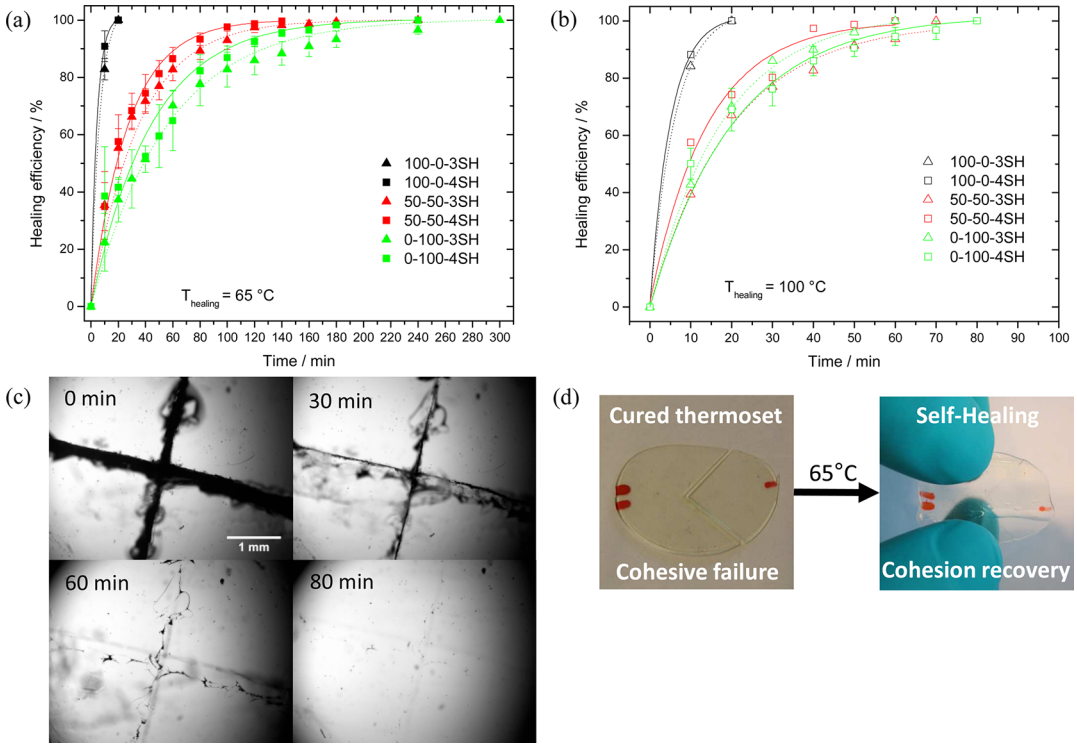

Figure 3. (a) Healing efficiency at 65 °C for the 3-SH (▲ and dotted line) and 4-SH (■ and full line) based materials. (b) Healing efficiency at 100 °C for the 3-SH (Δ and dotted line) and 4-SH (□ and full line) based materials. (c) Optical microscope pictures showing the cohesive healing for 0-100-4SH material at 100 °C as function of time. (d) Example of macroscopic cohesion recovery.

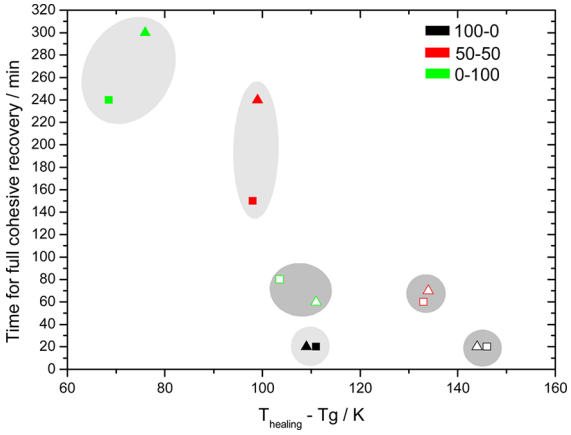

Figure 4. Specific healing time needed to reach 100% cohesive recovery at 65 °C (full symbols) and 100 °C (empty symbols) for 4-SH (■) and 3-SH (▲) based material as function of the difference between the healing temperature and the T_g.

difference between the T_g and the healing temperature, then, at least, the Epikote-3H material would have only shown cohesion recovery at 100 °C which is not the case. In general thermosets (rubberlike or not) do not present any thermal mending ability when the temperature is far above the T_g. Starting with a fully cross-linked network, in the present work the cleavage of the S−S bonds is responsible of a local network rupture and the healing reaction. If the thermoset network cannot be ruptured no macroscopic chains flow can be induced and no self-healing response could have been achieved.

As the investigated healing process in this material is related to the covalent bond exchange reaction, the overall dependence of the specific time for full cohesive recovery at a particular temperature clearly depends on the network cross-link density. In this sense, a denser network is achieved when 4-SH type of cross-linkers are used. This implies a higher probability for the polymeric chains to be in close contact and thus a higher probability for two disulfide bonds to come close enough allowing disulfide bonds exchange to occur. Added to this density parameter, the chain/network flexibility plays a major role in the self-healing response. When aromatic units are added the thermal mending ability is slowed down in comparison to a fully aliphatic network because of the higher chain/network rigidity and thus reduced mobility. This effect on the cohesion recovery is predominant for the fully aliphatic materials where both 3-SH and 4-SH systems exhibit a healing time of 20 min irrespective the healing temperature. When the chains rigidity is increased, the network cross-link density become the limiting factor for the healing kinetics. As it can be seen in Figure 4, this effect will be minimized when the healing temperature is sufficiently high and far above the T_g. The cohesive recovery is enhanced when the network density is high and chain mobility is high. Decreasing the network density does not really affect a flexible network but drastically hamper the cohesive recovery of a more rigid network. In order to minimize this effect coming from a less dense and more rigid network, the healing temperature needs to be increased. In any case, full thermal mending and network integrity recovery was achieved with all our materials containing disulfide bonds in their structure. As fast cohesion recovery is thus enhanced when difference between the healing temperature and the T_g is maximized, when the network flexibility is enhanced and when the network cross-link density is increased.

The results of the adhesion recovery experiments are presented in Figure 5 and show that all disulfide bond containing materials present a clear recovery of their initial

dx.doi.org/10.1021/am301879z | ACS Appl. Mater. Interfaces 2012, 4, 6280−6288

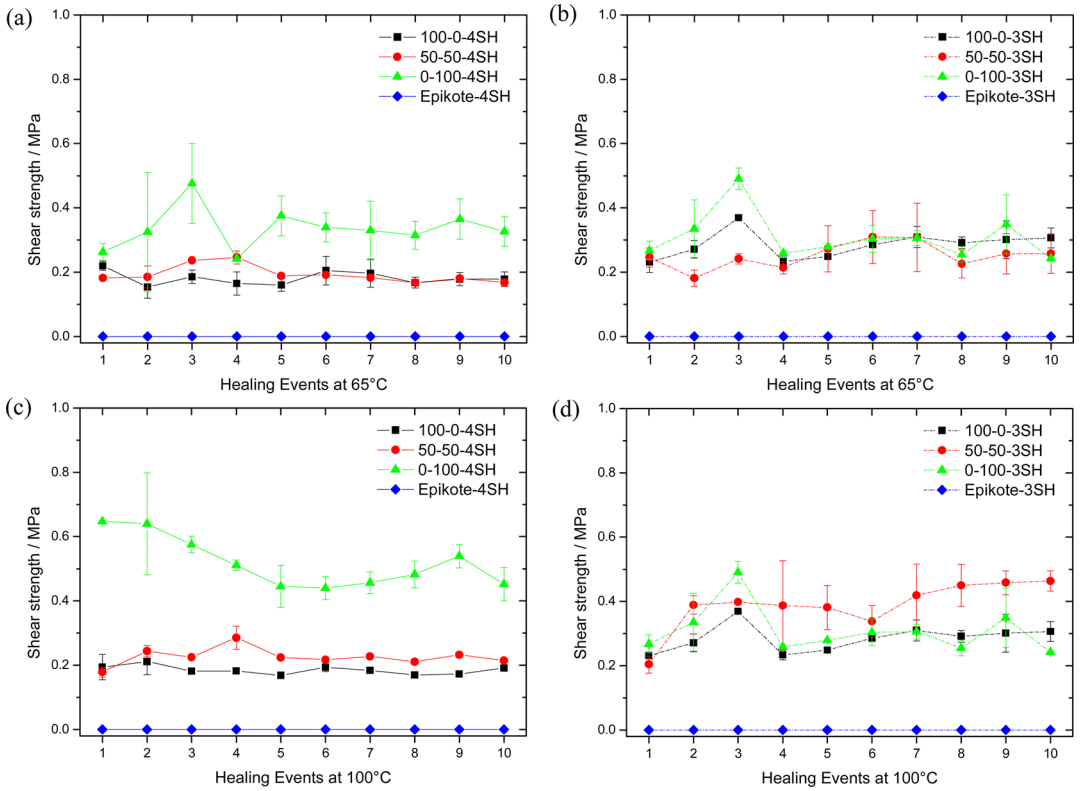

Figure 5. Adhesion recovery as function of the healing temperature and cross-linker type at 65 °C using (a) 4-SH or (b) 3-SH and at 100 °C using (c) 4-SH or (d) 3-SH.

adhesive properties. The values of first healing events on the plots are related to the first adhesion using pristine cured samples. Furthermore, all materials show the ability to multiple healing and no significant drop in healed adhesive strength with the number of healing cycles was observed. During lap shear test, all materials did show an adhesive failure mode. Using the 4-SH cross-linker the material using EPS70 presents the highest adhesive strength that is 2−3 times higher than the adhesive strength of EPS25 based material, irrespective of the healing temperature. The blended material (50−50) exhibits a slightly higher shear strength compared to the pure EPS25 material for a low healing temperature (Figure 5a) but this difference is reduced when the healing takes place at 100 °C (Figure 5c). Using the 3-SH cross-linker, pure EPS25, EPS70 or blended materials do not exhibit significant differences in their adhesive behavior. At a high healing temperature (Figure 5d), the materials present a better adhesion compare to the case of low healing temperature (Figure 5b). Epikote-4SH or Epikote-3SH based material did not show any adhesion or readhesion to the aluminum alloy, whatever the thermal treatment.

When the four-branched cross-linker is used, the healing temperature does not affect the elongation at rupture (Figure 6). These values slightly decrease during the first 5 healing events to stabilize at around 1% for the pure aliphatic and mixed (50−50) material. The ESP70 based thermoset show the same behavior with an elongation at rupture around 2.5%. When the trithiol is used as cross-linker, the elongation at rupture for the material healed at 65 °C fluctuates between 2 and 3%. At 100 °C, the materials behave slightly differently. The EPS25 based material does not change, the mixed material stabilized at 3%, whereas the pure EPS70-based material reaches 4% of elongation.

The dynamic bonding ability upon thermal activation implies that the molecular network is locally disrupted. The combination of a low T_g with covalent bonds disruption will allow macroscopic flow. The reference materials made using a polymer without disulfide bonds but with the same cross-linkers, did not show any postcuring cohesion or adhesion recovery. The dynamic bonds exchange based on disulfide bonds will be favored when two disulfide bonds are close enough. In this respect, the use of a short chain 4-branched cross-linker is thus more likely to result in a good healing behavior as it will increase the probability of reactive units in the backbone to come into contact with each other compared to a longer chain 3-branched cross-linker. The density of the produced material presented in Table 2 clearly exhibit higher values for the 4-SH based materials compare to the 3-SH ones. Moreover, chain flexibility will play an important role to favor the disulfide bond mobility. These two hypothesis are well in line with the cohesive healing results in which the 4-SH based network present the faster healing kinetics as well as the material based on aliphatic chain (EPS25). Decreasing the network cross-link density by using a cross-linker with longer chains and lowering the network connectivity results in a decreased healing efficiency at low temperatures. By increasing the network rigidity via incorporation of aromatic end-chain segments, the healing kinetics are hampered. Giving more energy to the system by increasing the healing temperature minimizes the negative effect of the network cross-link density as well as the negative effect of chain rigidity on the healing rate. In the same way, from an adhesive perspective, this induced chain mobility will allow a renewal of functional groups at the interface leading to the recovery of the adhesive properties. The material self-healing response is to be related to

dx.doi.org/10.1021/am301879z | ACS Appl. Mater. Interfaces 2012, 4, 6280−6288

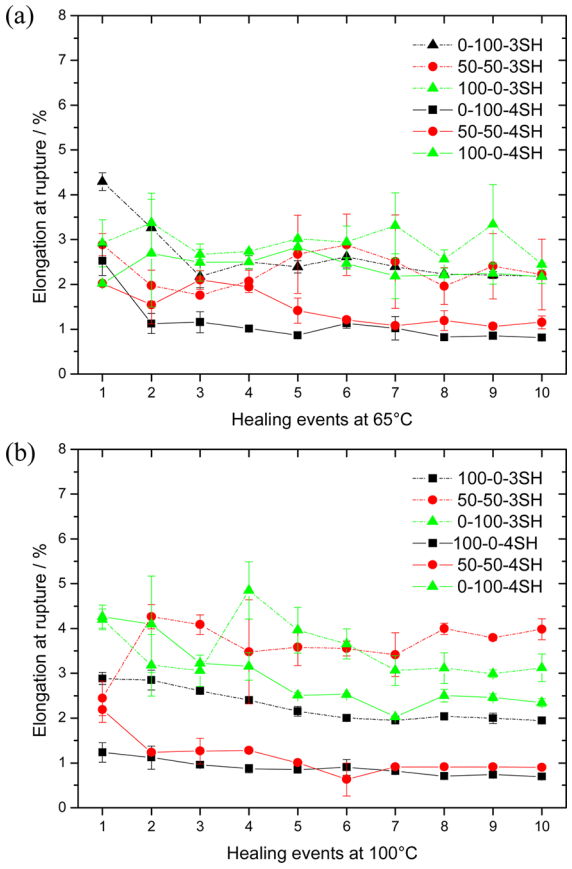

Figure 6. Elongation at rupture for 3-SH (dotted line) and 4-SH (full line) based composite as function on the healing events at (a) 65 and (b) 100 °C.

the presence of disulfide bonds. Canadell et al. experimentally proved, by producing a network where aliphatic epoxidized polysulfide was replaced by exactly the same polymer without any disulfide bonds that only in the presence of disulfide in such cross-linked network a self-healing response was obtained.[43] However according to the literature, the mechanism related to this self-healing concept is not well established and two potential reactions can be distinguished. The first one is related to the well-established thiol-disulfide exchange reaction which is observed in proteins. One can think of the case of a nonfully cross-linked network in which the presence of thiol pending functions could favor this reaction. This mechanism implies that unreacted/pending thiols are present in the material and moreover, that there is a suitable environment that allows the creation of thiolate anions. In our material the basic catalyst (DMAP) used to promote the ring-opening of the oxirane for the cross-linking reaction could also act as catalyst to create thiolate anions in the cured material upon heating. However, according to the infrared spectroscopy results presented in this study, no pending thiols can be detected once the materials are cured. This absence of pending thiols disfavors the thiol-disulfide exchange mechanism to explain the dynamic bonding ability of such systems. Moreover, after at least 10 healing cycles involving thermal treatment at 100 °C, we show that the adhesion recovery still occurs. If the healing mechanism was related to a nonfully cured sample, it would disappear or drastically decrease as function of the thermal treatment. The second mechanism involves an interchain disulfide bond exchange reaction leading to a covalent reversible cleavage of the disulfide bonds.[42−44,67,69,70] This so-called disulfide metathesis or opening of sulfur cross-link by rearrangement[43,67,70] implies the creation of thiyl radicals which then undergo exchange with other neighboring disulfides.[64,71] Further studies are needed to fully understand this mechanism and moreover the role of a possible catalytic activation of this dynamic bonds exchange reaction. Whatever the outcome of such mechanistic studies, the materials presented here show recovery of their (mechanical) integrity by re-establishing cohesion as well as their adhesive properties with regards to Al alloys show rather different responses as a function of the type of cross-linker used. These results clearly show that in the creation of intrinsic self-healing material based on dynamic bonding ability, the network cross-link density as well as the intrinsic chain rigidity and mobility are of paramount importance.

CONCLUSION

We have demonstrated that thermoset rubber materials containing disulfide bonds show cohesive and multiple adhesive healing ability once cured. Macroscopic flow induced by the reversible bond exchange is a good strategy to promote thermally triggered self-healing properties. The use of a four-branched or three-branched cross-linker affects the self-healing behavior and kinetics. The network density as well as the chain mobility have an impact on the material thermal healing efficiency. A dense network based on a four-branched cross-linker increases the healing properties of the network at low temperatures specifically when the resin contains flexible chains. Depending of the formulation, adhesive strength values between 0.18 and 0.52 MPa can be reached which are fully recovered over multiple failure-thermal healing cycles. This approach is an interesting route to create self-healing matrices for polymer-based multifunctional composite interfacial materials for microsystems application.[5]

ASSOCIATED CONTENT

Supporting Information

DSC data showing the glass transition for all samples investigated in this work, DSC data with isotherm at 120 °C, lap shear test sample images and dimension, and Cohesion recovery images. These materials are available free of charge via Internet via http://pubs.acs.org.

AUTHOR INFORMATION

Corresponding Author

*E-mail: U.Lafont@tudelft.nl. Tel: +31 15 278 86 21. Fax: +31 15 278 44 72.

Notes

The authors declare no competing financial interest.

ACKNOWLEDGMENTS

This research was carried out under project number M71.9.10381 in the framework of the Research Program of the Material innovation institute (M2i) (www.m2i.nl). The authors would like to thanks Dr. O. Klobes (Akzo Nobel Functional Chemicals) for providing the polysulfide materials together with technical support. M. Hegde is acknowledged for assistance in the thermal characterization tests.

REFERENCES

(1) van der Zwaag, S. *Self Healing Materials*; Springer: Dordrecht, the Netherlands, 2007.
(2) Blaiszik, B. J.; Kramer, S. L. B.; Olugebefola, S. C.; Moore, J. S.; Sottos, N. R.; White, S. R. *Annu. Rev. Mater. Res.* **2010**, *40*, 179−211.
(3) Cho, S. H.; White, S. R.; Braun, P. V. *Adv. Mater.* **2009**, *21*, 645−649.
(4) García, S. J.; Fischer, H. R.; van der Zwaag, S. *Prog. Org. Coat.* **2011**, *72*, 211−221.
(5) Lafont, U.; Zeijl, H. v.; van der Zwaag, S. *Microelectron. Reliab.* **2012**, *52*, 71−89.
(6) Brown, E. N.; White, S. R.; Sottos, N. R. *J. Mater. Sci.* **2004**, *39*, 1703−1710.
(7) Brown, E. N.; White, S. R.; Sottos, N. R. *Compos. Sci. Technol.* **2005**, *65*, 2474−2480.
(8) Brown, E. N.; White, S. R.; Sottos, N. R. *Compos. Sci. Technol.* **2005**, *65*, 2466−2473.
(9) Tian, W.; Wang, X.; Pan, Q.; Mao, Z. *Huagong Xuebao (Chin. Ed.)* **2005**, *56*, 1138−1140.
(10) Toohey, K. S.; White, S. R.; Sottos, N. R. In *Self-Healing Polymer Coatings*, Proceedings of the 2005 SEM Annual Conference and Exposition on Experimental and Applied Mechanics; Society for Experimental Mechanics: Bethel, CT, 2005; pp 241−244.
(11) Blaiszik, B. J.; White, S. R.; Sottos, N. R. In *Nanocapsules for Self-Healing Composites*, Proceedings of the SEM Annual Conference and Exposition on Experimental and Applied Mechanics; Society for Experimental Mechanics: Bethel, CT, 2006; pp 391−396.
(12) Yuan, L.; Liang, G.; Xie, J.; Li, L.; Guo, J. *Polymer* **2006**, *47*, 5338−5349.
(13) Hayes, S. A.; Jones, F. R.; Marshiya, K.; Zhang, W. *Composites, Part A* **2007**, *38*, 1116−1120.
(14) Toohey, K. S.; Sottos, N. R.; Lewis, J. A.; Moore, J. S.; White, S. R. *Nat. Mater.* **2007**, *6*, 581−585.
(15) Yin, T.; Rong, M. Z.; Zhang, M. Q.; Yang, G. C. *Compos. Sci. Technol.* **2007**, *67*, 201−212.
(16) Blaiszik, B. J.; Sottos, N. R.; White, S. R. *Compos. Sci. Technol.* **2008**, *68*, 978−986.
(17) Mookhoek, S. D.; Blaiszik, B. J.; Fischer, H. R.; Sottos, N. R.; White, S. R.; Van Der Zwaag, S. *J. Mater. Chem.* **2008**, *18*, 5390−5394.
(18) Blaiszik, B. J.; Caruso, M. M.; McIlroy, D. A.; Moore, J. S.; White, S. R.; Sottos, N. R. *Polymer* **2009**, *50*, 990−997.
(19) Liao, L. P.; Zhang, W.; Zhao, Y.; Li, W. J. *Chem. Res. Chin. Univ.* **2010**, *26*, 496−500.
(20) McIlroy, D. A.; Blaiszik, B. J.; Caruso, M. M.; White, S. R.; Moore, J. S.; Sottos, N. R. *Macromolecules* **2010**, *43*, 1855−1859.
(21) Wang, H. P.; Rong, M. Z.; Zhang, M. Q. *Prog. Chem.* **2010**, *22*, 2397−2407.
(22) Jin, H.; Mangun, C. L.; Stradley, D. S.; Moore, J. S.; Sottos, N. R.; White, S. R. *Polymer* **2012**, *53*, 581−587.
(23) Kirkby, E. L.; Michaud, V. J.; Manson, J. A. E.; Sottos, N. R.; White, S. R. *Polymer* **2009**, *50*, 5533−5538.
(24) Bergman, S. D.; Wudl, F. *J. Mater. Chem.* **2008**, *18*, 41−62.
(25) Wojtecki, R. J.; Meador, M. A.; Rowan, S. J. *Nat. Mater.* **2011**, *10*, 14−27.
(26) Goussé, C.; Gandini, A. *Polym. Int.* **1999**, *48*, 723−731.
(27) Gheneim, R.; Perez-Berumen, C.; Gandini, A. *Macromolecules* **2002**, *35*, 7246−7253.
(28) Chen, X.; Dam, M. A.; Ono, K.; Mal, A.; Shen, H.; Nutt, S. R.; Sheran, K.; Wudl, F. *Science* **2002**, *295*, 1698−1702.
(29) Zhang, Y.; Broekhuis, A. A.; Picchioni, F. *Macromolecules* **2009**, *42*, 1906−1912.
(30) Reutenauer, P.; Buhler, E.; Boul, P. J.; Candau, S. J.; Lehn, J. M. *Chem.—Eur. J.* **2009**, *15*, 1893−1900.
(31) Peterson, A. M.; Jensen, R. E.; Palmese, G. R. *Compos. Sci. Technol.* **2011**, *71*, 586−592.
(32) Chen, X.; Wudl, F.; Mal, A. K.; Shen, H.; Nutt, S. R. *Macromolecules* **2003**, *36*, 1802−1807.
(33) Kavitha, A. A.; Singha, N. K. *ACS Appl. Mater. Interfaces* **2009**, *1*, 1427−1436.
(34) Kavitha, A. A.; Singha, N. K. *Macromolecules* **2010**, *43*, 3193−3205.
(35) Cordier, P.; Tournilhac, F.; Soulié-Ziakovic, C.; Leibler, L. *Nature* **2008**, *451*, 977−980.
(36) Tournilhac, F.; Cordier, P.; Montarnal, D.; Soulié-Ziakovic, C.; Leibler, L. *Macromol. Symp.* **2010**, *291−292*, 84−88.
(37) Bosman, A. W.; Sijbesma, R. P.; Meijer, E. W. *Mater. Today* **2004**, *7*, 34−39.
(38) Beijer, F. H.; Sijbesma, R. P.; Kooijman, H.; Spek, A. L.; Meijer, E. W. *J. Am. Chem. Soc.* **1998**, *120*, 6761−6769.
(39) Groote, R.; Szyja, B. M.; Pidko, E. A.; Hensen, E. J. M.; Sijbesma, R. P. *Macromolecules* **2011**, *44*, 9187−9195.
(40) Piermattei, A.; Karthikeyan, S.; Sijbesma, R. P. *Nat. Chem.* **2009**, *1*, 133−137.
(41) Yuan, J.; Fang, X.; Zhang, L.; Hong, G.; Lin, Y.; Zheng, Q.; Xu, Y.; Ruan, Y.; Weng, W.; Xia, H.; Chen, G. *J. Mater. Chem.* **2012**, *22*, 11515−11522.
(42) Amamoto, Y.; Kamada, J.; Otsuka, H.; Takahara, A.; Matyjaszewski, K. *Angew. Chem., Int. Ed.* **2011**, *50*, 1660−1663.
(43) Canadell, J.; Goossens, H.; Klumperman, B. *Macromolecules* **2011**, *44*, 2536−2541.
(44) Yoon, J. A.; Kamada, J.; Koynov, K.; Mohin, J.; Nicolaÿ, R.; Zhang, Y.; Balazs, A. C.; Kowalewski, T.; Matyjaszewski, K. *Macromolecules* **2012**, *45*, 142−149.
(45) Varley, R. J.; van der Zwaag, S. *Acta Mater.* **2008**, *56*, 5737−5750.
(46) Kalista, S. J., Jr; Ward, T. C. *J. R. Soc. Interface* **2007**, *4*, 405−411.
(47) Varley, R. J.; van der Zwaag, S. *Polym. Int.* **2010**, *59*, 1031−1038.
(48) Varley, R. J.; Shen, S.; van der Zwaag, S. *Polymer* **2010**, *51*, 679−686.
(49) van der Zwaag, S.; van Dijk, N. H.; Jonkers, H. M.; Mookhoek, S. D.; Sloof, W. G. *Philos. T. R. Soc A* **2009**, *367*, 1689−1704.
(50) Klukovich, H. M.; Kean, Z. S.; Iacono, S. T.; Craig, S. L. *J. Am. Chem. Soc.* **2011**, *133*, 17882−17888.
(51) Connal, L. A.; Vestberg, R.; Hawker, C. J.; Qiao, G. G. *Adv. Funct. Mater.* **2008**, *18*, 3315−3322.
(52) Froimowicz, P.; Frey, H.; Landfester, K. *Macromol. Rapid Commun.* **2011**, *32*, 468−473.
(53) Ling, J.; Rong, M. Z.; Zhang, M. Q. *Polymer* **2012**, *53*, 2691−2698.
(54) Billiet, S.; Van Camp, W.; Hillewaere, X. K. D.; Rahier, H.; Du Prez, F. E. *Polymer* **2012**, *53*, 2320−2326.
(55) Wang, F.; Rong, M. Z.; Zhang, M. Q. *J. Mater. Chem.* **2012**, *22*, 13076−13084.
(56) Montarnal, D.; Capelot, M.; Tournilhac, F.; Leibler, L. *Science* **2011**, *334*, 965−968.
(57) Luo, X. F.; Ou, R. Q.; Eberly, D. E.; Singhal, A.; Viratyaporn, W.; Mather, P. T. *ACS Appl. Mater. Interfaces* **2009**, *1*, 612−620.
(58) Peterson, A. M.; Jensen, R. E.; Palmese, G. R. *ACS Appl. Mater. Interfaces* **2009**, *1*, 992−995.
(59) Peterson, A. M.; Jensen, R. E.; Palmese, G. R. *ACS Appl. Mater. Interfaces* **2010**, *2*, 1141−1149.
(60) Wilson, G. O.; Caruso, M. M.; Schelkopf, S. R.; Sottos, N. R.; White, S. R.; Moore, J. S. *ACS Appl. Mater. Interfaces* **2011**, *3*, 3072−3077.
(61) Sevier, C. S.; Kaiser, C. A. *Nat. Rev. Mol. Cell Biol.* **2002**, *3*, 836−847.
(62) Chujo, Y.; Sada, K.; Naka, A.; Nomura, R.; Saegusa, T. *Macromolecules* **1993**, *26*, 883−887.
(63) Kamada, J.; Koynov, K.; Corten, C.; Juhari, A.; Yoon, J. A.; Urban, M. W.; Balazs, A. C.; Matyjaszewski, K. *Macromolecules* **2010**, *43*, 4133−4139.
(64) Adhikari, B.; De, D.; Maiti, S. *Prog. Polym. Sci. (Oxford)* **2000**, *25*, 909−948.
(65) Wiita, A. P.; Ainavarapu, S. R. K.; Huang, H. H.; Fernandez, J. M. *Proc. Natl. Acad. Sci. U. S. A.* **2006**, *103*, 7222−7227.
(66) Ainavarapu, S. R. K.; Wiita, A. P.; Dougan, L.; Uggerud, E.; Fernandez, J. M. *J. Am. Chem. Soc.* **2008**, *130*, 6479−6487.

(67) Otsuka, H.; Nagano, S.; Kobashi, Y.; Maeda, T.; Takahara, A. *Chem. Commun.* **2010**, *46*, 1150−1152.
(68) Ma, Y.; Chechik, V. *Langmuir* **2011**, *27*, 14432−14437.
(69) Arisawa, M.; Suwa, A.; Yamaguchi, M. *J. Organomet. Chem.* **2006**, *691*, 1159−1168.
(70) Rajan, V. V.; Dierkes, W. K.; Joseph, R.; Noordermeer, J. W. M. *Prog. Polym. Sci. (Oxford)* **2006**, *31*, 811−834.
(71) Fairbanks, B. D.; Singh, S. P.; Bowman, C. N.; Anseth, K. S. *Macromolecules* **2011**, *44*, 2444−2450.